Auditory Neuroscience, 1996, Vol 2, pp. 145–157
Reprints available directly from the publisher
Photocopying permitted by license only

Receptor Potential of Outer Hair Cells Isolated from Base to Apex of the Adult Guinea-Pig Cochlea: Implications for Cochlear Tuning Mechanisms

SERENA PREYER, SABINE RENZ, WERNER HEMMERT, HANS-PETER ZENNER, and ANTHONY W. GUMMER

University of Tübingen, Department of Otorhinolaryngology, Section Physiological Acoustics and Communication, Silcherstrasse 5, 72076 Tübingen, Germany

(Received January 23, 1995; Accepted: October 17, 1995)

If the electromotility of outer hair cells (OHC) is to reduce the mechanical impedance of the cochlear partition, it must not only deliver a force of sufficient magnitude, but the force must be exerted at the correct moment in the stimulus cycle. The amplitude and phase of the receptor potential of OHCs in response to direct mechanical stimulation of the stereocilia bundle were measured for cells isolated from along the entire length of the adult guinea-pig cochlea. Irrespective of their place of origin, the frequency response of the receptor potential, for 20-nm stereociliary displacement per spectral point, was governed by the OHC electrical input impedance measured near the resting potential. The response was a low-pass filter with amplitude that decreased by 6 dB/oct and phase that lagged stereocilia displacement by 90°. The corner frequency of the response decreased exponentially from 546 Hz for the shortest OHC (20 μm) with an exponential length constant of 25 μm, or equivalently 0.58 oct per 10 μm increase of cell length. The tonotopy was achieved by an exponential decrease in the total specific conductance with increasing cell length, beginning at 66 pS/μm² for the shortest OHC; the specific capacitance was constant (2.0 μF/cm²). The corner frequency was 3–6 oct below the presumed place-frequency.

Key words: Outer hair cell, receptor potential, electrical input impedance, cochlear tuning, mammal

Corresponding author: Dr. S. Preyer, University of Tübingen, Department of Otorhinolaryngology, Section Physiological Acoustics and Communication, Silcherstraße 5, 72076 Tübingen, Germany

ALTHOUGH THE MECHANISM of cochlear tuning and sensitivity remains elusive, there is strong evidence that the outer hair cells (OHC) are a necessary ingredient (Brown and Nuttall, 1984; Dallos and Harris, 1978; Dolan and Nuttall, 1994) and that active, stimulus-induced length changes of the cell body are involved, producing forces on the cochlear partition sufficient to partially cancel frictional losses (Ashmore, 1987; Brownell, *et al.*, 1985; Dallos *et al.*, 1991, 1993; Evans *et al.*, 1991; Huang and Santos-Sacchi, 1993; Santos-Sacchi, 1989, 1991, 1992; Santos-Sacchi and Dilger, 1988; Zenner, 1986; Zenner *et al.*, 1985, 1987). Not only must these forces be of sufficient magnitude, but they must have the correct phase. For example, if the OHC were to produce a maximal contractile force at the moment when the direction of the basilar membrane (BM) motion changed from scala vestibuli to scala tympani then the OHC would actively "brake" BM motion—the effective damping of the cochlear partition would be increased, resulting in a loss of tuning. This moment must be determined, amongst other things, by the phase of the electromechanical force relative to the displacement of the stereocilia. This phase difference is unknown. The somatic displacement of isolated OHCs, driven by changes of the transmembrane potential (Dallos *et al.*, 1991, 1993; Huang and Santos-Sacchi, 1993), is capable of following sinusoidal extracellular field potentials (Brownell *et al.*, 1985; Dallos *et al.*, 1991, 1993; Dallos and Evans, 1995; Evans *et al.*, 1991; Reuter and Zenner, 1990; Reuter *et al.*, 1992; Zenner *et al.*, 1987) and intracellularly injected current under voltage clamp (Ashmore, 1987; Santos-Sacchi, 1989, 1991, 1992), cycle-by-cycle up to high frequencies, without either attenuation or phase delay up to at least 22 kHz (Dallos and Evans, 1995). Therefore, if there is no phase delay between somatic displacement and transmembrane potential, as implied by the data of Dallos and Evans (1995), then for an isolated OHC any phase difference between the electromechanical force and stereocilia displacement must be due to: i) the phase of the receptor potential relative to stere-

ocilia displacement and ii) the phase of the contractile force relative to somatic displacement. The former is known only for OHCs isolated from the apical part of the cochlea (Preyer *et al.*, 1994) and the latter, which is specified by the mechanical impedance of the cell, is unknown.

Therefore, the aim of this paper is to determine experimentally the amplitude and phase, relative to stereociliary displacement, of the receptor potential of OHCs isolated from along the entire length of the adult guinea-pig cochlea. This information is particularly important for cells from the basal region where the cochlea is exquisitely tuned (Evans, 1972; Dallos and Harris, 1978) and the demands on the OHCs greatest.

METHODS

The experimental methods are similar to those described previously (Preyer *et al.*, 1994), but with modifications essential for obtaining intact cells from the basal half of the cochlea.

Cell Preparation

Pigmented, adult guinea-pigs with positive Preyer's reflex (Preyer, 1900) were decapitated after cervical dislocation, their temporal bones removed, placed in standard Hanks' balanced salt solution (HBSS) and chilled in ice. The composition of the HBSS was (in mM): 137 NaCl, 5.4 KCl, 0.34 Na_2HPO_4, 0.44 KH_2PO_4, 0.81 $MgSO_4.7H_2O$, 1.25 $CaCl_2$, 5.5 D-Glucose, 4.2 $NaHCO_3$ (Seromed). After 30 min. the cochlea was opened, stria vascularis and tectorial membrane were peeled from the underlying epithelium, which was then loosened from the bone and placed in four separate groups corresponding to each of the cochlear turns. Each group was transferred to 150 µL of HBSS for the purpose of either enzymatic digestion or mechanical dislocation and recording; the exact protocol depended on the cochlear turn. For cells from the apical half of the cochlea, enzyme digestion was not used and the osmolarity of the HBSS was 300 mOsm (Preyer *et al.*, 1994). In this case, the cells were simply isolated by gentle mechanical dislocation by aspirating in an Eppendorf pipette. For cells from the basal half of the cochlea, however, it was necessary to include an intermediate step of enzymatic digestion—in this case the HBSS contained 1 mg/mL type IV collagenase (Sigma) in which the epithelia were placed for 10 min. before being transferred to 150 µL of collagenase-free HBSS for mechanical dislocation by aspiration; the osmolarity of the solutions was 320 mOsm, adjusted with 4M NaCl. Although collagenase aided dislocation of OHCs from the supporting cells and also enabled a giga-seal with little or no application of a negative pressure to the cell wall, the lifetime of the isolated cells was approximately halved. Therefore, with the exception of control experiments, enzymatic digestion was avoided in the apical half of the cochlea. After aspiration, the isolated cells settled and adhered to an uncoated glass coverslip, without the addition of adhesive agents. The difference in osmolarity of the HBSS bathing solution used for cells from the basal and apical halves of the cochlea corresponded approximately to the endolymphatic osmolarity gradient reported *in vivo* by Sterkers *et al.* (1984). Control experiments showed that the membranes of apical OHCs tended to lose their bifringence in 320 mOsm HBSS, taking on a wrinkled appearance, and that basal OHCs swelled in 300 mOsm HBSS. The pH was 7.4, adjusted with 1M NaOH and the room temperature was controlled at 20–23°C. Cells were viewed under an inverted microscope (Leitz Labovert) with a total magnification of 788x with a Zeiss 63x oil immersion objective. The microscope was coupled to a video system with contrast enhancement (Hamamatsu, 2400); the image of a contacted cell was recorded continuously (Sony U-matic Videocasette recorder). The length and diameter of the cell in the unpatched condition were measured from the video-screen.

Whole-Cell Recording

Whole-cell recordings were made in current clamp (Hamill *et al.*, 1981) using a List EPC-7 amplifier and soda-glass pipettes filled with standard internal K^+ solution (in mM): 140 KCl, 2 $MgCl_2$, 11 EGTA, 1 $CaCl_2$, 10 HEPES). All data were corrected for the frequency response of the patch-clamp amplifier (Preyer *et al.*, 1994). The electrode resistance in extracellular fluid was typically 1.5–2 MΩ and the series resistance in whole-cell configuration 3–4 MΩ (estimated from the measured electrical input impedance of the patched cell). Electrodes were designed to have low resistance in order to maximize the recording bandwidth. Cells were patched apical to their nucleus and basal from the subcuticular space, with a tendency to patch in the apical half of this region to ensure mechanical stabilization during hair-bundle deflection. Resting potentials are given as zero-current potentials after correction for the liquid junction potential (–4 mV). Only cells with a resting potential negative to –39 mV were used for the experiments. The majority of recordings were stable for 10–15 minutes, with some stable up to 30 minutes.

Properties of the Pseudorandom Noise Stimulus

Frequency responses were measured with pseudorandom noise stimuli instead of sinusoidal stimuli to minimize the measurement time. The function generator of a spectrum analyzer (AD 3525, A&D Co., Japan) was used for producing noise stimuli. The stimulus and response signals were averaged in the time domain. Although the stimulus signal was derived from a random process, the same sample function was employed for each stimulus presentation used to form an average

frequency response. The frequency response was given simply as the Fourier transform of the time-averaged response relative to the Fourier transform of the time-averaged stimulus. A different sample function was used for subsequent evaluation of a frequency response.

A stimulus sample function was derived from a zero-mean Gaussian random process, N(t), which was simulated as a sequence of harmonically related sinusoids with equal amplitudes, a, but random phases, Φ_i ($i = 1, \ldots, i_{max}$), uniformly distributed on the interval $[0,2\pi]$; namely,

$$N(t) = a \sum_{i=1}^{i_{max}} \sin(2\pi f_0 \, it + \Phi_i)$$

where f_0 is the fundamental frequency. In our application, N(t) was sampled at 512 equally spaced instants. In order to minimize aliasing errors and to ensure a flat amplitude spectrum, the function generator automatically set the maximum number of spectral components, i_{max}, to 200, rather than to the theoretically allowable Nyquist value of 256. That is, the amplitude of each spectral component with frequency from f_0 to the user-specified maximum frequency, $f_{max} = 200f_0$, was equal to a, and as such was a sample function from a band-limited, zero-mean Gaussian (white-noise) process. For 512 time samples, a was on average 31.4 dB below the user-specified maximum voltage output (±1 V). The variance, σ^2, of a random process with zero-mean can be estimated in the usual manner as the integral of the power spectral density function, S(f), over all frequencies (Wozencraft and Jacobs, 1965). Since the power in a sinusoid of amplitude, a, is equal to $\frac{1}{2}a^2$, we have $S(f) = \frac{1}{2}a^2/f_0$ for every spectral component. Then, $\sigma^2 = \frac{1}{2}a^2 f_{max}/f_0 = \frac{1}{2}a^2 i_{max}$. Therefore, for 200 spectral points, the standard deviation of N(t), was estimated as $\sigma = 10a$. An example of a sample function from N(t) is illustrated in Fig. 1 for $f_{max} = 500$ Hz and $a = 0.0243$ V. Also shown is the normalized histogram of sample values, together with the probability density function of a Gaussian random variable. A X^2-test ($p < 0.01$, 9 degrees of freedom) showed that the sample function was indeed drawn from a zero-mean Gaussian random process; the sample standard deviation of 0.245 V was approximately equal to the theoretical value of $10a = 0.243$ V.

Since the noise stimulus was to be used to estimate the frequency response of the linear component of the system, it was important to choose the maximum voltage output of the signal generator so that the system was rarely, if ever, driven into its nonlinear operating region. Because the sample functions were drawn from a Gaussian random process, N(t), the probability that a sample value, $N(\tau)$, at some instant, τ, exceeded a given value, N_0, is given as:

$$\text{Prob}[N(\tau) > N_0] = \tfrac{1}{2} \, \text{erfc}(N_0 / \sqrt{2}\sigma)$$

where erfc(.) is the complementary error function (Wozencraft and Jacobs, 1965). Three cases are of interest. First, 68% of the sample values were expected to lie within the range of $\pm\sigma$, which is equal to $\pm 10a$ for 200 spectral points. Second, the probability that $N(\tau)$ was greater than 4.1σ is 1/512, meaning that only one of the 512 sample values, on average, was expected to exceed 4.1σ, or $41a$ for 200 spectral points. In practice, it was found that only one of the 512 sample values, on average, exceeded $32a$. Third, the probability that at some instant all spectral components had the same phase and, therefore, produced a sample value of magnitude $i_{max}\, a$, is given as $\frac{1}{2}$ erfc($\sqrt{i_{max}}$), which for 200 spectral points is infinitesimally small (2.7×10^{-89}). In practice, it was found that the sample values did not exceed $37a$.

Hair-Bundle Stimulation

Deflection of the hair bundle was achieved with a short, rigid borosilicate glass pipette with a tip diameter of about 5 μm, driven by a low-voltage piezoelectric crystal (Type PSt 15/4/15 Pickelmann GmbH, Munich). After registration of a stable resting membrane potential, the stimulus pipette was placed against the apical region of the stereociliary bundle and its position adjusted so as to maximize the receptor potential for low-frequency sinusoidal stimulation. The frequency response of the stimulus pipette was flat from 0 Hz to 5 kHz (±1 dB), with resonant frequency near 9 kHz, as measured with a laser Doppler velocimeter (Polytec OFV-302). The electrical

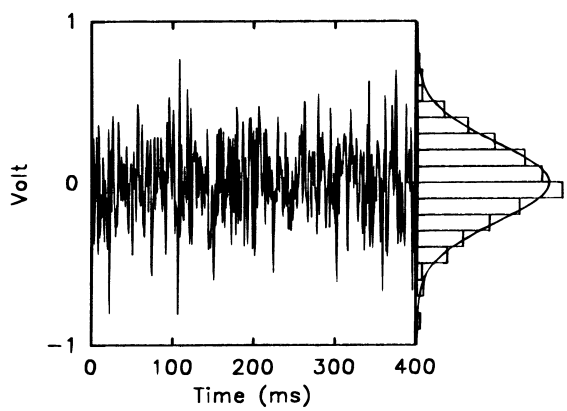

FIGURE 1 **Sample function from the zero-mean, Gaussian random process used for stimulus generation.** The function contains 512 sample values equally spaced in time. The random process was produced using a series of 200 sinusoids with frequencies equally spaced from 2.5 Hz to 500 Hz, each with amplitude of 0.0243 V and random phases uniformly distributed on $[0,2\pi]$. The histogram of sample values contains 20 bins of equal width on the interval from −1 V to +1 V. The histogram is normalized to unity area; the largest bin has value of 1.8. The curve drawn through the histogram is the probability density function of a Gaussian random variable with mean and standard deviation equal to their sample values of −0.0013 V and 0.2446 V, respectively; ($X^2 = 3.25$).

signal driving the piezoelectric crystal was either a 1 Hz sinusoid (multifunction synthesizer, HP 89049) or band-limited zero-mean white noise generated by a spectrum analyzer (AD 3525, A&D Co., Japan). The amplitude for sinusoidal stimulation was 1 μm peak-to-peak to produce a maximal, saturated receptor potential. The displacement noise signal contained 200 equally spaced spectral points, each with amplitude of 20 nm, giving a standard deviation for the noise of 200 nm. The noise process was sampled at 512 equally spaced instants. On average, 68% of the sample values were within ±200 nm and one of the 512 values was greater than 640 nm, but always less than 740 nm. Therefore, most displacement values were within the linear operating range of the input-output function of the receptor potential (Preyer *et al.*, 1994).

Electrical Input Impedance

The electrical input impedance of the patched cell was evaluated by measuring the change in membrane potential in response to intracellular injection of band-limited, zero-mean white-noise current with the cell clamped to zero current (Preyer *et al.*, 1994). The current noise signal contained 200 equally spaced spectral points, each with amplitude of 8 pA, giving a standard deviation for the noise of 80 pA. The noise process was sampled at 512 equally spaced instants. On average, 68% of the sample values were within ±80 pA and one of the 512 values was greater than 256 pA, but always less than 296 pA.

The ratio of measured voltage to injected current was corrected for the frequency response of the patch-clamp amplifier, both in amplitude and phase. For this purpose, a test circuit with known impedance, Z_T, was substituted for the patched hair cell. The test circuit was a simplified model of the electrical input impedance of a patched cell, having a resistance (4 MΩ) in series with a parallel combination of a resistance (50 MΩ) and a capacitance (39 pF). The voltage, V_T, at the amplifier output was measured in response to a current, I_T, at the input of the test circuit. Simple circuit analysis shows that to correct the impedance data for the frequency response of the amplifier, the ratio V/I measured in the patched-cell configuration need only be multiplied by a factor $I_T Z_T / V_T$. The analysis assumes that Z_T is much smaller than the input impedance of the amplifier. For frequencies up to 5 kHz, this correction factor resembled a low-pass filter with corner frequency of 2.1 kHz.

The electrical input impedance of the cell was estimated by fitting the measured amplitude and phase responses to those of an impedance formed by a resistance (the series resistance of the electrode), in series with the parallel combination of a resistance and a capacitance (the presumed electrical input impedance of the isolated cell), (Santos-Sacchi, 1989; Preyer *et al.*, 1994). The respective amplitude and phase functions were fitted to the impedance data with the Marquardt-Levenberg algorithm (SigmaPlot).

Data Acquisition and Statistics

The spectrum analyzer (AD 3525, A&D Co., Japan) was used to provide the stimulus signal sample, average, store and analyze the data. Both the noise stimulus and the response signal were averaged in the time domain. For a maximum frequency of 500 Hz, the average contained responses to 8 stimulus presentations; the number of presentations was doubled for each doubling of maximum frequency. The averaging time was 6–8 sec. Complete frequency responses were formed by superimposing the average frequency responses derived from successively wider stimulus bands; the maximum frequencies were 500, 1000, 2000 and 5000 Hz. There were always 200 spectral points per frequency band, equally spaced on a linear frequency axis. The first frequency was $f_{max}/200$. A complete frequency response was constructed in approximately 60 sec. This paradigm enabled high resolution and also provided checks on the reproducibility of the responses.

Frequency responses and scatter diagrams were fitted in the least-mean-square sense with the Marquardt-Levenberg algorithm (SigmaPlot). The parameter estimates of a fit are quoted as mean ± s.d. Statistical significance of i) parameter estimates (t-test), ii) differences between parameter estimates (t-test) or iii) correlation coefficients was evaluated at the 99% level.

RESULTS

Complete frequency responses were obtained from 46 OHCs and of these the electrical input impedance was measured for 42. The cell length ranged from 20 μm for the most basal segment to 87 μm for the most apical segment of the cochlea. OHCs with lengths as small as 15 μm were observed, but successful recordings were not achieved. Resting potentials ranged from –78 mV to –40 mV (–64 ± 10 mV; N = 46). None of the parameters reported here were found to be correlated with the resting membrane potential. It was difficult to obtain complete sets of data from the shortest OHCs, as should be appreciated from the comparison of the long OHC and the short OHC shown in Figure 2. First, the longest stereocilia of a hair bundle were much smaller for short OHCs (2 μm) than for the long OHCs (8 μm), meaning that it was more difficult to attain or maintain suitable contact with the hair bundle. Although trial experiments using a fluid jet rather than a glass probe yielded relatively more cells with a detectable receptor potential, the fluid jet was not used for frequency-response experiments because of the uncertainty of the frequency response of the force delivered to the hair bundle, particularly at high frequencies where fluid viscosity and mass must become appreciable. Control experiments showed that the increased yield with the fluid jet was not due to mechanical damage by the glass probe, but rather to the geometry of the experimental set-up restricting the

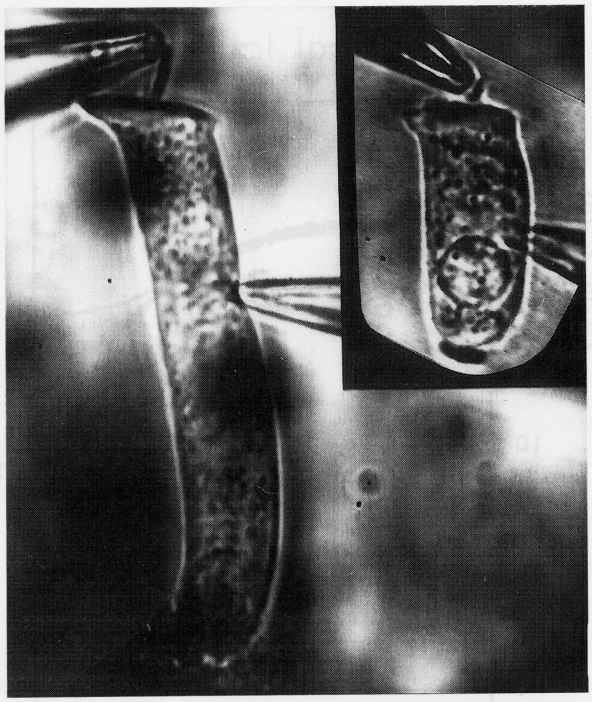

FIGURE 2 **Comparison of the recording configuration for a short (30 μm) and a long (71 μm) OHC.**

stimulus probe to a narrow range of approach angles to the hair bundle. All data are for stimulation in the direction of the longest stereocilia. Second, the length of cell membrane along which a receptor potential was found was comparatively short for the basally located OHCs: if the cells were patched too high in the region of the subcuticular space, no receptor potential was observed, possibly because of a disturbance of the transduction apparatus; if patched too low towards the nucleus, the recording was mechanically unstable. Third, smaller OHCs did not adhere as readily to the glass cover-slip, thus precluding their being patched.

The most useful indicator of a mechanically and electrically stable preparation was a non-random phase response for noise stimulation. In the absence of controlled stimulation, the amplitudes of the membrane potential resembled wideband noise filtered by a low-pass filter, consistent with the power spectral density analysis of Denk and Webb (1992) for frog sacculus hair cells, but the phase was randomly distributed between ±180° (Fig. 8a, b). Therefore, when using noise stimuli, only the phase can be used as a stability criterion.

Frequency Response of the Receptor Potential

Irrespective of their cochlear origin, the frequency response of the receptor potential relative to displacement of the hair bundle resembled that of a first-order low-pass filter: i) the amplitude was constant up to a corner frequency, above which it decreased at 6 dB/oct (Fig. 3a, 4a) and ii) the phase was zero at low frequencies, decreased to –45° at a frequency corresponding to the corner frequency of the amplitude response and tended to –90° at higher frequencies (Fig. 3b, 4b). The frequency responses illustrated in Figs. 3 and 4 are for two OHCs of different lengths.

For the quantification of the relevant frequency-response parameters, the amplitude and phase data were fitted separately with the amplitude and phase responses of a first-order low-pass filter; namely with the respective fit functions:

$$A = A_0 / [1 + (f/f_{3dB})^2]^{1/2}$$

and

$$\Phi = \Phi_0 - \arctan(f/f_{45°})$$

where the low-frequency asymptotic amplitude, A_o, and phase, Φ_o, together with the 3-dB frequency, f_{3dB}, and the 45°-frequency, $f_{45°}$, were estimated with the Marquardt-Levenberg algorithm (SigmaPlot). The estimated f_{3dB} and $f_{45°}$ frequencies were not significantly different, implying that the recorded frequency responses are due to the stimulus and not to random fluctuations of the membrane potential. Therefore, in future discussion the mean value of f_{3dB} and $f_{45°}$ will be referred to as the corner frequency. In these examples the corner frequencies were 70 Hz and 239 Hz, respectively, for lengths of 80 μm and 38 μm.

Electrical Input Impedance

Since the frequency response of the receptor potential for long OHCs (70–90 μm) from the apical region of the cochlea has been shown (Preyer *et al.*, 1994) to be governed predominantly by the electrical input impedance of the cell, the impedance of the patched OHC was determined after measuring the receptor-potential data. This was achieved by recording the change in membrane potential as a result of intracellular injection of bandlimited, zero-mean white-noise current, with the cell clamped to zero current. Results for a short and a long OHC are shown in Figures 3 and 4, respectively. The amplitude and phase of the electrical input impedance, after correction for the series electrode resistance, had a low-pass filter form with corner frequencies of 70 Hz and 200 Hz, respectively, for the long and the short OHC. These values are not significantly different from those of the receptor potential.

Corner Frequency

In general, irrespective of cochlear origin, the frequency response of the receptor potential was defined almost exclusively by the electrical input impedance of the OHC. This is illustrated in Figure 5 where the corner frequen-

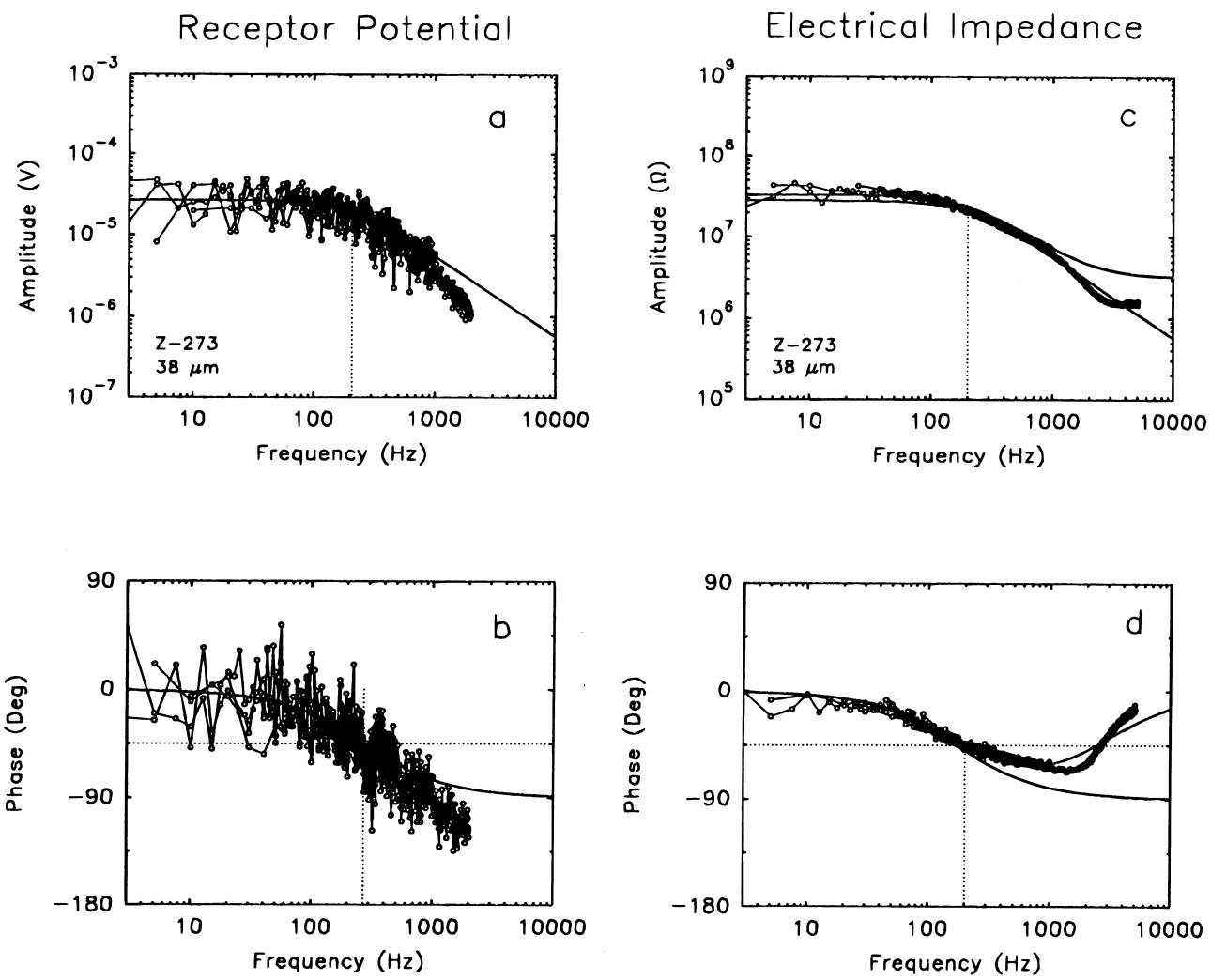

FIGURE 3 **Receptor potential and electrical input impedance of an OHC of length 38 μm isolated from the first-to-second turn of the adult guinea-pig cochlea.** The hair bundle was stimulated in the direction of the longest stereocilia with bandlimited, zero-mean white noise with 20 nm per frequency point and 200 frequency points per overlapping frequency band; there were three bands extending respectively to 500, 1000 and 2000 Hz. The receptor-potential response (*a*, *b*) resembles a first-order low-pass filter, as indicated by the full lines, which were derived by fitting the data to the ideal amplitude and phase functions (see text). Fitted filter values: $A_o = 27 \pm 1$ μV, $\Phi_o = 1 \pm 3$ deg, $f_{3dB} = 207 \pm 16$ Hz, $f_{45°} = 270 \pm 35$ Hz. The estimates for f_{3dB} and $f_{45°}$ are not significantly different and Φ_o is not significantly different from zero, as required of a first-order low-pass filter. The increased amplitude slope and additional phase lag above approximately 1 kHz occurred because it was not possible to fully correct for the frequency response of the patch-clamp system above 1.6 kHz. The electrical input impedance (*c*, *d*) was measured near the resting potential with the cell clamped to zero current. The impedance was derived from the change in membrane potential resulting from intracellular injection of bandlimited, zero-mean white-noise current with amplitude of 8 pA per frequency point and 200 points per overlapping frequency band. Upper lines in *c* and *d*: fitted line assuming that the impedance of the patched OHC is given by the series resistance, R_S, of the electrode in series with the parallel combination of a resistance, R_i, and capacitance, C_i, which represent the input impedance of the isolated OHC (*ie* cell without electrode). Lower lines in *c* and *d*: electrical input impedance of the isolated OHC (*ie* after correcting for the series electrode resistance); the result is $R_S = 3.2 \pm 0.1$ MΩ, $R_i = 28.2 \pm 0.2$ MΩ, $C_i = 28 \pm 1$ pF. Resting potential: –68 mV.

cies of the receptor potential (N = 46) and electrical input impedance (N = 42) are collected. The corner frequencies are plotted on a logarithmic axis because of cochlear tonotopy. The length axis is linear rather than logarithmic because for the linear axis the data were randomly distributed about the regression lines, whereas this was not the case for a logarithmic presentation. The data show a well-defined, monotonic decrease in corner frequency with increasing cell length. The two data sets can be accurately described by regression lines with almost identical parameters. For the receptor potential, the exponential decrease of the corner frequency with cell

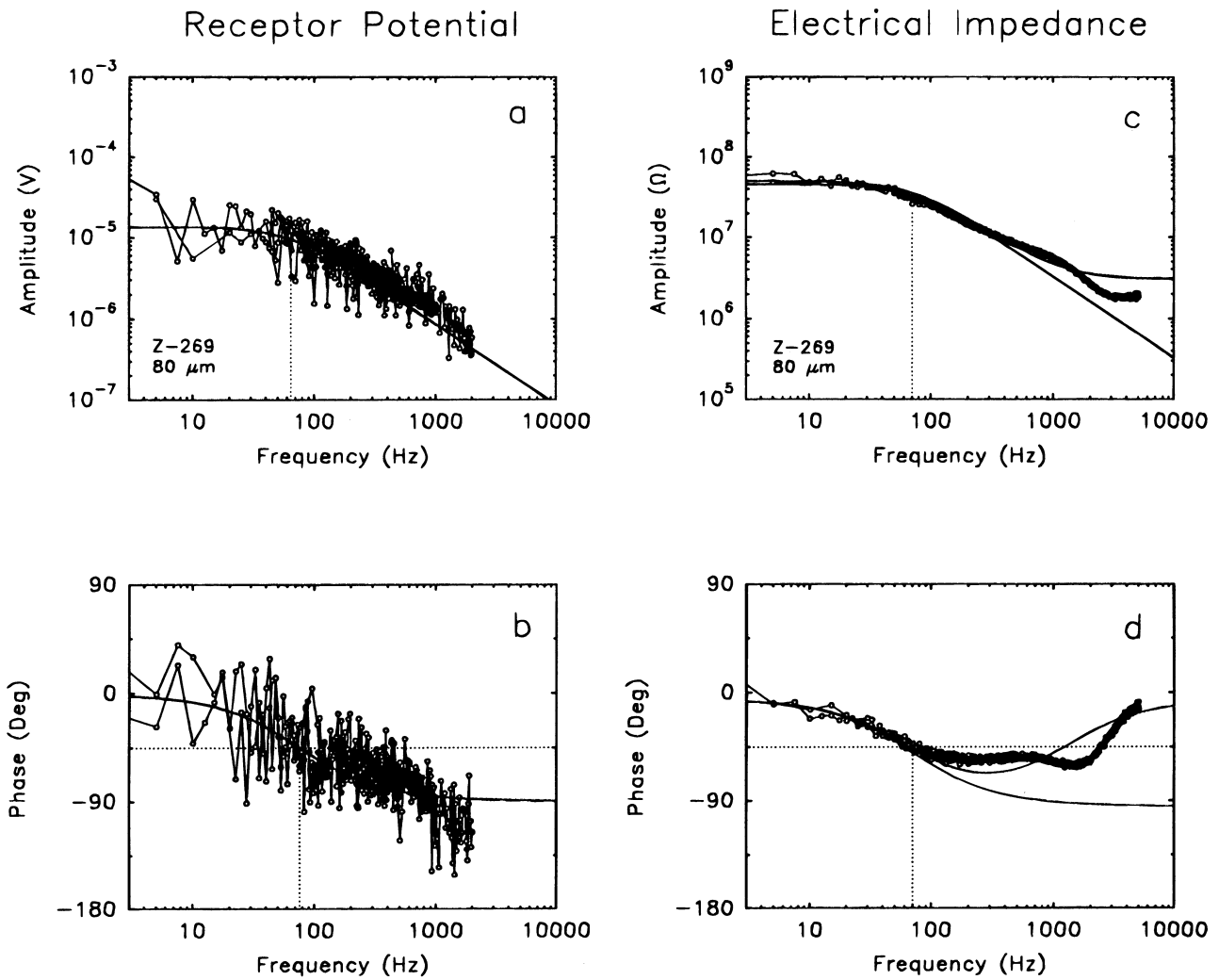

FIGURE 4 **Receptor potential and electrical input impedance of an OHC of length 80 μm isolated from the fourth turn of the adult guinea-pig cochlea.** Details as for Fig. 3. Fitted filter values: $A_o = 13.5 \pm 0.9$ μV, $\Phi_o = -0.9 \pm 3.2$ deg, $f_{3dB} = 64 \pm 7$ Hz, $f_{45°} = 76 \pm 14$ Hz. The estimates for f_{3dB} and $f_{45°}$ are not significantly different and Φ_o is not significantly different from zero, as required of a first-order low-pass filter. $R_S = 3.3 \pm 0.1$ MΩ, $R_i = 46.4 \pm 0.3$ MΩ, $C_i = 49 \pm 2$ pF. Resting potential: –41 mV.

length, L, was estimated as 1211 exp(-L/25) Hz; the value of 25 μm in the exponent will be referred to as the exponential length constant. In other words, the corner frequency for the receptor potential decreased by 0.58 oct. per 10 μm increase of cell length, beginning at 546 Hz for the shortest recorded OHC of length 20 μm. Therefore, if the extremes of cell length were derived from OHCs from the extremes of the cochlea, the corner frequencies for the apical-most and basal-most OHCs were about 2.6 oct and 6.2 oct. below their respective place frequencies.

Electrical Input Conductance and Capacitance

The decrease of corner frequency with increasing cell length was correlated with increasing resistance and capacitance of the cell. Although both parameters were dependent on the surface area of the cell, the density of conducting channels appeared to be larger for the shorter OHCs. This is illustrated in Figures 6 and 7, where not only are the conductances and capacitances collected, but also their specific values. The specific conductance and capacitance were calculated by dividing the absolute values by the surface area, assuming a cylinder of height equal to the cell length, L, and without taking account of the apical surface of the cell (Housley and Ashmore, 1992). The diameter of the cell was independent of its length and ranged from 8.3 μm to 12.5 μm (10 ± 1 μm). Surface area was calculated from the cell's dimensions, not from the mean dimensions of all cells. The measured specific conductances and capacitances give an indication of the density of conducting channels and the charge concentration near the resting potential. The conductance

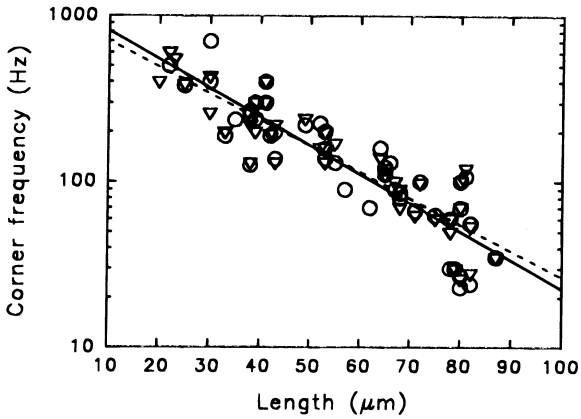

FIGURE 5 **Corner frequency of the receptor potential (circles) and the electrical input impedance (triangles) of isolated OHCs as a function of their length.** Shortest cells are from the basal and longest cells from the apical segments of the cochlea. Linear regression lines for the receptor potential (full line) and electrical input impedance (broken line), with logarithmic frequency axis, have respective slopes of 0.058 ± 0.005 oct/μm and 0.053± 0.004 oct/μm, intercept of 546 ± 27 Hz and 491 ± 24 Hz at 20 μm, and correlation coefficients (r) of –0.89 (N = 46) and –0.91 (N = 42). The slopes are equivalent to exponential length constants of 25 ± 2 μm and 27 ± 2 μm, respectively. These regression lines are not significantly different, implying that the frequency response of the receptor potential is governed by the electrical input impedance of the cell. No attempt has been made to separate data points for visual presentation purposes.

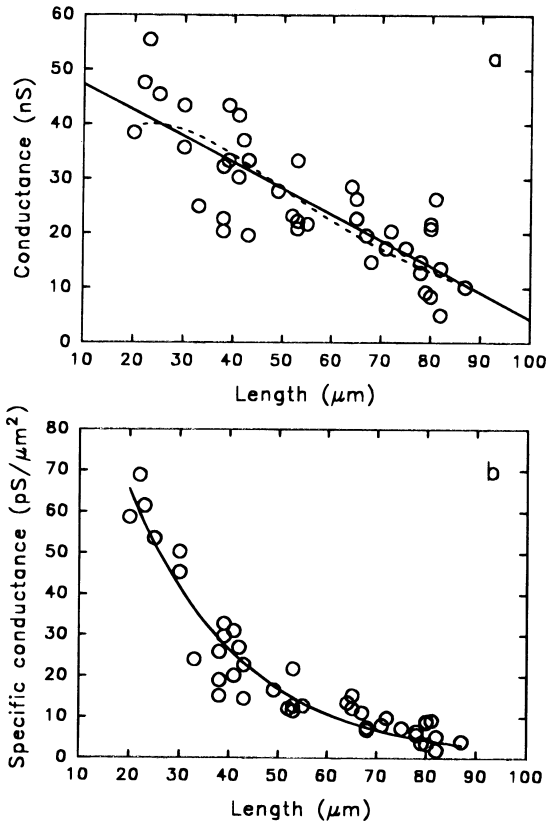

FIGURE 6 **OHC electrical input conductance (*a*) and specific conductance (b), measured near the resting potential, for cells of different length (N = 42).** The straight regression line in *a* has slope of –0.48 ± 0.05 nS/μm and conductance of 43 ± 2 nS for a 20-μm OHC (r = –0.82). The exponential regression curve in *b* has length constant of 22 ± 1 μm, and value of 66 ± 6 pS/μm² at 20 μm. The larger values of specific conductance for short OHCs implies either that the density of conducting channels was larger for cells located more basally in the cochlea or that they possessed channels with larger conductivity. The broken line in *a* is the regression curve assuming that the conductance, G_i, is proportional to the cell length, L, multiplied by a specific conductance with exponential dependence on cell length: G_i = (4.55 ± 0.51) L exp(–L/β) nS, where β = 24 ± 1 μm is not significantly different to the length constant for the specific conductance. However, this fit cannot be statistically distinguished from the straight line regression.

decreased in direct proportion to cell length, with slope of 0.48 nS/μm (Fig. 6a), and the specific conductance, G_{SP}, decreased exponentially from 66 pS/μm² for the shortest OHC of length 20 μm (Fig. 6b). The dependence of specific conductance on cell length means either that the concentration of conducting channels is larger for the smaller OHCs or that channels with higher conductivity are present in these basally located cells. The capacitance increased in direct proportion to cell length by 0.45 pF/μm (Fig. 7a); however, the specific capacitance was independent of cell length with value 2.0 μF/cm² (Fig. 7b), implying that the charge concentration was the same for all OHCs. (If the condition for statistical significance of the correlation coefficient for specific capacitance versus cell length were relaxed from 99% to 95%, a tendency for increased specific capacitance with decreasing length would be concluded, which was mainly evident below 40 μm). The exponential length constant for the specific conductance was 22 μm, which is not significantly different (t-value = 2.2) from that of the corner frequency (25 μm), implying that the dependence of corner frequency on cell length was governed by the specific conductance.

Low-Frequency Receptor Potential

The amplitude of the receptor potential at low frequencies tended to increase with cell length (0.46 ± 0.09 μV/μm; r = 0.64), or equivalently 23 dB between the cochlear extremes (not illustrated). Although this increase is consistent with the finding of larger resistances for longer OHCs, as predicted by Housley and Ashmore (1992), a direct comparison cannot be made because for all OHCs the stimulus was a constant displacement rather than a constant rotation of the hair bundle. Thus, if transduction current is proportional to angular displacement of the stereocilia, then the effective stimulus for the shortest OHCs (2-μm stereocilia) would have been about four times larger than for the longest OHCs (8-μm stereocilia).

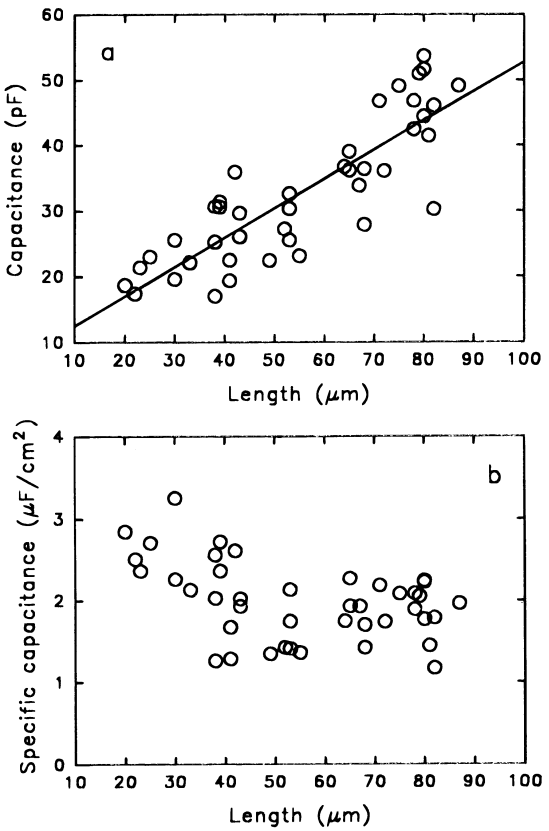

FIGURE 7 **OHC electrical input capacitance (*a*) and specific capacitance (*b*), measured near the resting potential, for cells of different length (N = 42).** The straight regression line in *a* has slope of 0.45 ± 0.04 pF/μm and capacitance of 17 ± 2 pF for a 20-μm OHC (r = 0.85). The specific capacitance was not correlated (r = 0.43) with cell length (1.99 ± 0.47 μF/cm²), implying that the charge density was the same for all cells along the cochlea.

Effect of Damaging the Hair Bundle

That the frequency response of the receptor potential was governed exclusively by the electrical input impedance was demonstrated by controlled mechanical damage to the hair bundle. Damage was produced by moving the tip of the stimulus probe back and forth through the hair bundle with the micromanipulator. The result is illustrated in Figure 8. Damage of the hair bundle abolished the receptor potential (Fig. 8a,b) without affecting the electrical input impedance (Fig. 8c,d). The variations in amplitude of the membrane potential, but not the phases, could still be fitted by the amplitude response of a first-order low-pass filter. This filter had the same corner frequency as the receptor potential but its amplitude was attenuated by 23 dB. Most importantly, after damage, the phases were random and bore no relation to the amplitudes, implying that the amplitudes were simply due to fluctuations of the membrane potential.

DISCUSSION

These experiments have shown that the receptor potential of isolated OHCs, measured near their resting potential, varies systematically along the cochlea and that its frequency response is shaped by the electrical input impedance of the cell.

Electrical Input Impedance

The electrical input impedance was characterized by a first-order low-pass filter, with conductance and capacitance that varied with cell length, the conductance decreasing by 0.48 nS/μm from 43 nS at 20 μm, and the capacitance increasing by 0.45 pF/μm from 17 pF at 20 μm. On average, the corner frequencies decreased from 491 Hz for the shortest cells to 41 Hz for the longest cells; the measured range was 27–613 Hz. These values are in complete agreement with those reported by Housley and Ashmore (1992) using the customary method of electrical stimulus steps (–0.59 nS/μm, 0.47 pF/μm, with 38 nS and 17 pF at 20 μm; average corner frequencies decreasing from 270 Hz to 88 Hz and measured range of 53–1060 Hz).

In further agreement with their data, the specific capacitance was independent of cell length (2.0 μF/cm²). A similar value of specific capacitance (1.9 μF/cm²) was reported by Housley and Ashmore (1992) and, as pointed out in their paper, is higher than typical values for lipid membranes because of the voltage-dependent capacitance of OHCs. Nevertheless, the capacitance values were not correlated with the resting membrane potential, presumably because most (83%) were within a narrow range (±10 mV) of the mean (–64 mV).

Although the dependence of specific conductance on cell length was also similar to that reported by Housley and Ashmore (1992), we chose to fit our data with an exponential function, $a_1 \exp(-L/a_2)$, instead of the hyperbolic function, $a_1 + a_2/L$. There were two reasons for this choice. First, for long cells the exponential function tends asymptotically to zero, whereas the hyperbolic function tends to a_1, which for both data sets was (significantly) negative and, therefore, nonsensical. The parameters for the hyperbolic function for their data are $a_1 = -16.9$ pS/μm² and $a_2 = 1450$ pS/μm and for our data are $a_1 = -15.5 \pm 1.9$ pS/μm² and $a_2 = 1663 \pm 82$ pS/μm. The parameters from the two data sets are in good agreement. (Their parameter values were derived by dividing their linearly fitted conductance data ($G_{in} = -0.585\ L + 50.1$ nS) by the cell surface area ($2\pi rL$), using for the cell radius, r, their quoted mean value of 5.5 μm). Second, we found an exponential dependence of corner frequency on cell length which, for the observed constancy of specific capacitance, suggested an exponential dependence of specific conductance on length. It should be emphasized, however, that although there were physical reasons for fitting the specific-conductance data with an exponential rather than a hyperbolic function, there was

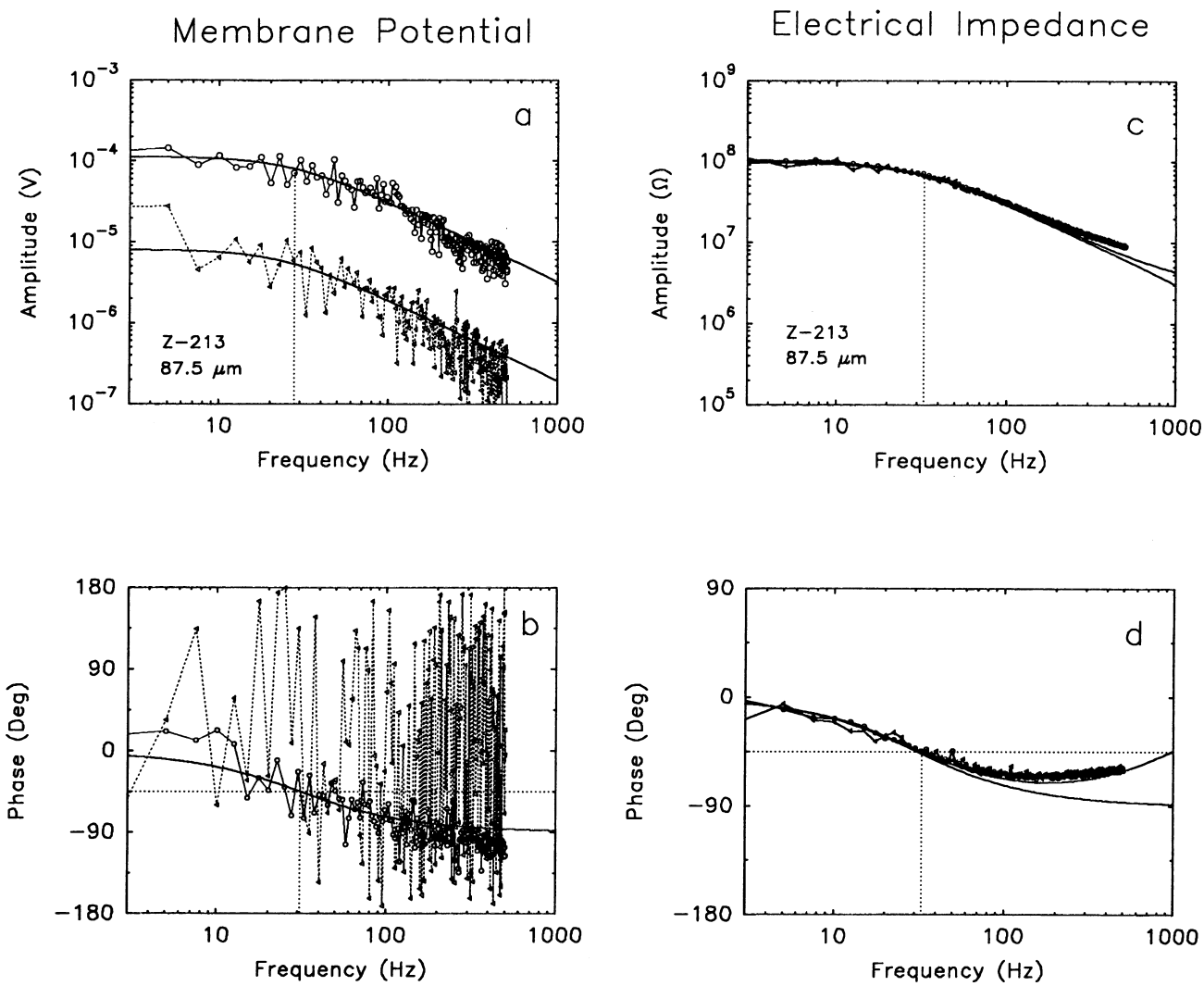

***FIGURE 8* Controlled mechanical damage of the hair bundle abolished the receptor potential (*a,b*) and had no detectable effect on the electrical input impedance (*c,d*).** The resting potential was not affected (–68 mV). The frequency response of the receptor potential before damage (circles) was fitted by the parameters of a first-order low-pass filter: $A_o = 113 \pm 4$ μV, $f_{3dB} = 28 \pm 1.6$ Hz, $\Phi_o = -0.78 \pm 7.8$ deg., $f_{45°} = 31 \pm 11$ Hz. After damage (triangles), the phase of the membrane potential fluctuations was random, indicating the absence of a stimulus-controlled change of the membrane potential; nevertheless, the amplitude fluctuations were described with a first-order low-pass filter with $A_o = 8 \pm 0.6$ μV, $f_{3dB} = 24 \pm 2.5$ Hz. The corner frequencies before and after damage were not significantly different, consistent with the electrical input impedance being unaffected by stereociliary damage. For the membrane potential fluctuations, points at 2.5 Hz (not shown) and 5 Hz have been omitted from the amplitude fit for the damaged case because their relatively large values suggested that they derived from an additional noise source, presumably 1/f background noise. For the electrical input impedance, $R_S = 3.9 \pm 0.2$ MΩ, $R_i = 98 \pm 1$ MΩ, $C_i = 49 \pm 2$ pF. Number of spectral points: 200.

no statistical basis for this choice. Finally, an exponential fit to the data of Housley and Ashmore (1992), their Fig. 4b, yielded a length constant of 19 ± 1 μm, and specific conductance of 54 ± 5 pS/μm² at 20 μm (not illustrated); again, these values are not significantly different from our values.

The dependence of specific conductance, but not specific capacitance, on cell length means that the larger corner frequency for shorter OHCs is due to either a larger concentration of conducting channels or to channels with larger conductivity, rather than to a reduction of the surface area of the cell. Clearly, if there were no concentration gradient, then for the same channel species the conductance and capacitance would both change in direct proportion to surface area, thus maintaining a constant corner frequency. Quantitatively, if the same channel species were active near the resting potential irrespective of cell length, then according to the expo-

nential dependence (Fig. 6b), to achieve the 4.5 oct. range of corner frequencies, a 20-μm OHC must express a 23 times greater concentration of conducting channels than a 90-μm OHC.

Comparison With In-Vivo Conditions

In general, the receptor potentials measured under these isolated cell conditions were lower than found for OHCs *in-vivo* (Dallos, 1985; Kössl and Russell, 1992). Based on the results of control experiments and with sufficient experience in preparing the OHCs, we will argue in this section that the difference was mainly due to the efficiency of coupling the stimulus probe to the stereocilia rather than to damage to the stereocilia.

The saturating value of the receptor potential, which was not considered in detail in this experimental series, was shown in an earlier report (Preyer *et al.*, 1994) to range between 0.4 mV and 5.2 mV (mean 1.5 mV) for cells of length 70–90 μm. Control experiments in the present series showed that the saturating receptor potentials, evaluated with 1-Hz sinusoidal stimulation, were approximately twice as large when using a fluid jet as stimulus instead of a glass probe. When using the fluid jet, the values compared with the AC receptor potentials of OHCs in the basal (Kössl and Russell, 1992) and apical (Dallos, 1985) turns of the *in-vivo* guinea-pig cochlea, as well as in the organotypic culture of the neonatal mouse cochlea (Russell and Richardson, 1987); the reported values ranged typically between 4 mV and 10 mV. Moreover, in another series of control experiments, mechanical damage to the hair bundle was shown not only to cause an overall loss of receptor-potential amplitude, but also to cause the phase to vary randomly between ±180° (Fig. 8b). The electrical input impedance was exceedingly robust, remaining unaffected by the assault on the hair bundle. Therefore, the frequency content of the randomly fluctuating membrane potential was still given by the electrical input impedance. Finally, provided the resting potential remained stable, there was never evidence of fatigue, either in the response to sinusoidal stimuli (1 Hz) or in response to high-frequency noise stimulation. Based on these control experiments, it is suggested that the region of the hair bundle stimulated by the glass probe was too localized to ensure opening of the normal contingent of transducer channels and that any disturbance to the integrity of the hair bundle was minimal.

There was no evidence that the receptor potential adapted to the noise stimulus. In response to an excitatory force step, the receptor current and potential of mouse OHCs adapt with a time constant of about 6 ms., matching the time constant for mechanical relaxation of the hair bundle (Kros *et al.*, 1992; Russell *et al.*, 1989; 1992). In other words, the adaptation process acts as a first-order high-pass filter with f_{3dB} of about 27 Hz. Therefore, if mechanical relaxation and electrical adaptation to the noise stimulus were occurring in the present experiments, it would have been evident as a phase lead of 90° at very low frequencies, rather than the observed phase of zero.

Several of the electrical, mechanical and chemical conditions present in the cochlea cannot be reconstituted for an isolated hair cell surrounded by artificial perilymph, which may explain the small receptor potentials. In particular, the endocochlear potential, or its equivalent, is not available, so that the driving potential for the transducer current is reduced to about one half of its *in vivo* value (Johnstone and Sellick, 1972; Ashmore and Meech, 1986). The electrical input impedance of the OHC is influenced by loading due to the electrical input impedance of the organ of Corti (Dallos, 1984), as well as by the mechanical input impedances of the organ of Corti and the OHC (Mountain and Hubbard, 1994).

Parameters of the Frequency Response

Three parameters of the frequency-response of the OHC receptor potential and their systematic variation along the cochlea influence the efficacy of OHC electromotility as a cochlear tuning mechanism: i) the low-frequency amplitude, ii) the corner frequency, iii) the asymptotic phase lag of 90°. Since the transmembrane potential is the stimulus for synchronous electromotility (Dallos *et al.*, 1991, 1993), the observation of increasing corner frequency with basal location is an essential feature of OHCs from a tonotopically organized cochlea. This demand has been met partially by increasing the specific conductance of the OHC membrane with basal position in the cochlea. Whether this has been achieved at the expense of low-frequency gain cannot be decided conclusively until simultaneous measurements of stereocilia displacement and receptor current or potential are made. Although for a given bundle-rotation the gain is expected to decrease with increasing membrane conductance (Housley and Ashmore, 1992), it is not known whether, for constant stereocilia displacement, this can be compensated by the larger rotation of the shorter hair bundle of basally located OHCs. Moreover, the kinetics of basally located OHCs does not appear capable of keeping pace with the high-frequency demands of that region of the cochlea, where the corner frequency was as much as 6 oct. below the characteristic frequency, as opposed to only 3 oct. for OHCs from the apex of the cochlea. For a membrane filter with slope of 6 dB/oct. 6 oct. amounts to an amplitude attenuation of 36 dB relative to the low-frequency value. Not only is the drive to the electromotor thereby severely compromised, but such a relatively low corner frequency means that the phase lag, relative to hair-bundle displacement, is 90° for the frequency region relevant to enhanced cochlear tuning by the electromechanical action of the OHCs.

To understand the functional relevance of a phase lag of 90°, consider the dynamics of a point on the BM for a

sinusoidal fluid pressure with a stimulus frequency that is characteristic for that cochlear place. If the tectorial membrane is elastic, maximum displacement of the BM into scala vestibuli causes deflection of the OHC stereocilia in the excitatory direction (Rhode and Geisler, 1967) and a depolarizing receptor potential with maximum occurring 90° later in the cycle, when the BM is crossing the zero-displacement position from scala vestibuli towards scala tympani. At this moment, BM velocity is maximal and the fluid friction force, which is proportional to velocity, is maximal and directed against the BM towards scala vestibuli. A depolarizing receptor potential causes OHC contraction (Mammano and Ashmore, 1993), which is in-phase with the receptor potential (Dallos and Evans, 1995). If the OHC is elastic, the resultant contractile force is also in-phase with the receptor potential. Consequently, the maximal contractile force on the BM acts at the same moment and in the same direction as the fluid friction force. Therefore, instead of OHC contraction actively amplifying BM motion, it actively attenuates it—the OHC actively "brakes" the motion of the BM.

Based on these mechanoelectrical properties of isolated OHCs, one must conclude that electromotility alone is not sufficient to guarantee enhanced cochlear tuning. An additional mechanism, such as a resonant tectorial membrane (Allen, 1980; Mammano and Nobili, 1993; Zwislocki 1980) or extracellular potential gradients (Dallos and Evans, 1995), is required to provide the appropriate amplitude and phase conditions.

ACKNOWLEDGEMENTS

We are extremely grateful for the technical assistance of M. Hoβ. Supported by the Deutsche Forschungsgemeinschaft, SFB 307, Teilprojekt C10; SR is supported by a doctoral studentship from the Fortüne-Programm, University of Tübingen.

REFERENCES

Allen, J. B. (1980). Cochlear micromechanics—A physical model of transduction. *J. Acoust. Soc. Am. 68*, 1660–1670.

Ashmore, J. F. (1987). A fast motile response in guinea-pig outer hair cells: the cellular basis of the cochlear amplifier. *J. Physiol. 388*, 323–347.

Ashmore, J. F. and Meech, R. W. (1986). Ionic basis of membrane potential in outer hair cells of guinea pig cochlea. *Nature 322*, 368–371.

Brown, M. C. and Nuttall, A. L. (1984). Efferent control of cochlear inner hair cell responses in the guinea-pig. *J. Physiol. 354*, 625–646.

Brownell, W. E., Bader, C. R., Bertrand, D. and de Ribaupierre, Y. (1985). Evoked mechanical responses of isolated cochlear outer hair cells. *Science 227*, 194–196.

Dallos, P. (1984). Some electrical circuit properties of the organ of Corti. II. Analysis including reactive elements. *Hear. Res. 14*, 281–291.

Dallos, P. (1985). Response characteristics of mammalian cochlear hair cells. *J. Neurosci. 5*, 1591–1608.

Dallos, P. and Evans, B. N. (1995). High-frequency motility of outer hair cells and the cochlear amplifier. *Science 267*, 2006–2009.

Dallos, P. and Harris, D. (1978). Properties of auditory nerve responses in absence of outer hair cells. *J. Neurophysiol. 41*, 365–383.

Dallos, P., Evans, B. N. and Hallworth, R. (1991). Nature of the motor element in electrokinetic shape changes of cochlear outer hair cells. *Nature 350*, 155–157.

Dallos, P., Hallworth, R. and Evans, B. N. (1993). Theory of electrically driven shape changes of cochlear outer hair cells. *J. Neurophysiol. 70*, 299–323.

Denk, W. and Webb, W. W. (1992). Forward and reverse transduction at the limit of sensitivity studied by correlating electrical and mechanical fluctuations in frog saccular hair cells. *Hear. Res. 60*, 89–102.

Dolan, D. F. and Nuttall, A. L. (1994). Basilar membrane movement evoked by sound is altered by electrical stimulation of the crossed olivocochlear bundle. *Abs. 17th Ann. Midwinter Research Meeting Assoc. Res. Otolaryngol.*, P356.

Evans, B. N., Hallworth, R. and Dallos, P. (1991). Outer hair cell electromotility: The sensitivity and vulnerability of the DC component. *Hear. Res. 52*, 288–304.

Evans, E. F. (1972). The frequency response and other properties of single fibres in the guinea-pig cochlear nerve. *J. Physiol. 226*, 263–287.

Hamill, O. P., Marty, A., Neher, A., Sakmann, B. and Sigworth, F. J. (1981). Improved patch clamp technique for high resolution current recording from cells and cell-free membrane patches. *Pflügers Arch. 391*, 85–100.

Housley, G. D. and Ashmore, J. F. (1992). Ionic currents of outer hair cells isolated from the guinea-pig cochlea. *J. Physiol. 448*, 73–98.

Huang, G. and Santos-Sacchi, J. (1993). Mapping the distribution of the outer hair cell motility voltage sensor by electrical amputation. *Biophys. J. 65*, 2228–2236.

Johnstone, B. M. and Sellick, P. M. (1972). The peripheral auditory apparatus. *Qu. Rev. Biophys. 5*, 1–57.

Kössl, M. and Russell, I. J. (1992). The phase and magnitude of hair cell receptor potentials and frequency tuning in the guinea pig cochlea. *J. Neurosci. 12*, 1575–1586.

Kros, C. J., Rüsch, A. and Richardson, G. P. (1992). Mechano-electrical transducer currents in hair cells of the cultured neonatal mouse cochlea. *Proc. R. Soc. Lond. B 249*, 185–193.

Mammano, F. and Ashmore, J. F. (1993). Reverse transduction measured in the isolated cochlea by laser Michelson interferometry. *Nature 365*, 838–841.

Mammano, F. and Nobili, R. (1993). Biophysics of the cochlea: Linear approximation. *J. Acoust. Soc. Am. 93*, 3320–3332.

Mountain, D. C. and Hubbard, A. E. (1994). A piezoelectric model of outer hair cell function. *J. Acoust. Soc. Am. 95*, 350–354.

Preyer, W. Th. (1900). Die Seele des Kindes. Beobachtungen über die geistige Entwicklung des Menschen in den ersten Lebensjahren. 5th edition, Th. Griebens Verlag, Leipzig, p. 57.

Preyer, S., Hemmert, W., Pfister, M., Zenner, H.-P. and Gummer, A. W. (1994). Frequency response of mature guinea-pig outer hair cells to stereociliary displacement. *Hear. Res. 77*, 116–124.

Reuter, G. and Zenner, H.-P. (1990). Active radial and transverse motile responses of outer hair cells in the organ of Corti. *Hear. Res. 43*, 219–230.

Reuter, G., Gitter, A. H., Thurm, U. and Zenner, H.-P. (1992). High frequency radial movements of the reticular lamina induced by outer hair cell motility. *Hear. Res. 60*, 236–246.

Rhode, W. S. and Geisler, C. D. (1967). Model of the displacement between opposing points on the tectorial membrane and reticular lamina. *J. Acoust. Soc. Am. 42*, 185–190.

Russell, I. J. and Richardson, G. P. (1987). The morphology and physiology of hair cells in organotypic cultures of the mouse cochlea. *Hear. Res. 31*, 9–24.

Russell, I. J., Kössl, M. and Richardson, G. P. (1992). Nonlinear mechanical responses of mouse cochlear hair bundles. *Proc. R. Soc. Lond. B 250*, 217–227.

Russell, I. J., Richardson, G. P. and Kössl, M. (1989). The responses of cochlear hair cells to tonic displacements of the sensory hair bundle. *Hear. Res. 43*, 55–70.

Santos-Sacchi, J. (1989). Asymmetry in voltage-dependent movements of isolated outer hair cells from the organ of Corti. *J. Neurosci. 9*, 2954–2962.

Santos-Sacchi, J. (1991). Reversible inhibition of voltage-dependent outer hair cell motility and capacitance. *J. Neurosci. 11*, 3096–3110.

Santos-Sacchi, J. (1992). On the frequency limit and phase of outer hair cell motility: Effects of the membrane filter. *J. Neurosci. 12*, 1906–1916.

Santos-Sacchi, J. and Dilger, J. P. (1988). Whole cell currents and mechanical responses of isolated outer hair cells. *Hear. Res. 35*, 143–150.

Sterkers, O., Ferrary, E. and Amiel, C. (1984). Inter- and intra-compartmental osmotic gradients within the rat cochlea. *Am. J. Physiol. 247*, F602–606.

Wozencraft, J. M. and Jacobs, I. M. (1965). Principles of Communication Engineering. John Wiley & Sons, Inc., New York.

Zenner, H.-P. (1986). Motile responses in outer hair cells. *Hear. Res. 22*, 83–90.

Zenner, H.-P., Zimmermann, U. and Schmitt, U. (1985). Reversible contraction of isolated mammalian cochlear hair cells. *Hear. Res. 18*, 127–133.

Zenner, H.-P., Zimmermann, U. and Gitter, A. H. (1987). Fast motility of isolated mammalian auditory sensory cells. *Biochem Biophys. Res. Commun. 149*, 304–308.

Zwislocki, J. J. (1980). Symposium on cochlear mechanics: Where do we stand after 50 years of research? *J. Acoust. Soc. Am. 67*, 1679–1685.